Advanced Steel Construction – Vol. 22 No. 2 (2026) 198–207
DOI:10.18057/IJASC.2026.22.2.6

NUMERICAL STUDY ON STIFFENED CONCRETE-FILLED DOUBLE STEEL TUBE SQUARE COLUMNS BEHAVIOUR

Mohamed Ghannam [1, *] and Md Kamrul Hassan [2]

[1] *Associate professor in Structural Engineering Departement, Faculty of Engineering, Mansoura University, Mansoura, Dakahlia 35516, Egypt*

[2] *Seniour Lecturer in Fire Safety Engineering, School of Engineering, Design and Built Environment, Western Sydney University, Penrith, NSW 2751, Australia*

* *(Corresponding author: E-mail: m.ghannam@mans.edu.eg)*

A B S T R A C T

Nowadays, more research has been done to investigate the behaviour of concrete filled double steel tube (CFDT) columns owing to the numerous advantages over concrete-filled steel tube (CFST) columns. Very few studies have focused on the behaviour of stiffened CFDT columns. This research gap is aimed to be covered in this paper, by studying the behaviour of CFDT columns under axial loads using different stiffener profiles that are welded to the inner and outer tubes. The performance of square-stiffened CFDT columns is investigated using the finite element (FE) method. Three types of stiffeners were studied: rectangular, inclined, and tie stiffeners. The verified FE model is used to study the effect of different parameters on the behaviour of stiffened CFDT columns. The results show that using tie stiffeners give the most increase in the ultimate axial load capacity by more than 15%. A simplified analytical model is presented to predict the axial load capacity of stiffened CFDT columns using tie stiffeners.

A R T I C L E H I S T O R Y

Received: 25 June 2025
Revised: 2 January 2026
Accepted: 2 January 2026

K E Y W O R D S

Stiffened concrete filled double;
Steel tube columns;
Load capacity;
Stiffeners;
Finite element model;
Analytical model

1. Introduction

Concrete-filled double steel tube (CFDT) and concrete-filled double-skin tube (CFDST) columns represent advanced composite structural elements that are increasingly preferred in construction over conventional concrete-filled steel tube (CFST) columns due to their superior performance characteristics. A CFDST column comprises two concentrically placed steel tubes, with the annular space between them filled with concrete, leaving the central core void. This configuration yields lighter structures with enhanced ductility, strength, cyclic performance, and fire resistance [1-7]. The cross-sectional shapes of the inner and outer tubes can be varied, including circular-in-square, square-in-square, or circular-in-circular arrangements [8].

Initially, under loading, an interaction is formed between the inner steel tube and the concrete ring because the lateral expansion of the steel is greater than that of the concrete (a result of different Poisson's ratios) and inversely a gap is formed between outer steel tube and concrete. However, interaction between inner tube and concrete diminishes as the concrete enters the elasto-plastic stage. In the later loading stage and due to increasing strain in concrete interaction is formed between outer tube and concrete [2, 9].

The structural behavior of CFDST columns can be significantly improved by filling the central void core with concrete, resulting in a CFDT column. The solid concrete core not only substantially increases the cross-section's load capacity but also helps delay the outward and inward local buckling of the inner tube [10]. A key advantage of CFDT over CFDST columns is their superior fire resistance, primarily attributed to the heat sink effect provided by the concrete core, which can enhance fire resistance by up to 36% Romero et al. [1]

Interaction between the steel tube and the concrete core is a critical parameter influencing the overall behavior of CFST, CFDST, and CFDT composite columns. A primary strategy for enhancing structural performance is the incorporation of stiffeners welded to the steel tube, which promote confinement and bonding. The use of stiffeners in composite structures, particularly those utilized in offshore applications like wind turbine masts and steel towers, has been identified as a vital solution for mitigating problems associated with excessive weight and high cost [11, 12]

Stiffeners allow for the reduction of the steel tube thickness, leading directly to reductions in both structural weight and material cost. Numerous studies have demonstrated that employing binding bars or welding bars in CFST columns markedly enhances concrete confinement, increases axial load capacity, improves ductility, and delays elastic local buckling [13-16]

The application of rectangular rib stiffeners is also highly effective [17-21], with Tao et al. [18] and Tao et al. [19] showing they increase load capacity and postpone local buckling. These findings underscore that existing design codes may not accurately predict the load capacity of stiffened columns, a point further supported by the introduction of novel designs like the catty-cornered propped concrete-filled steel tube, which demonstrated increased ultimate load capacity. Singh et al. [22]. In fact, previous research indicates that most design codes overlook the beneficial effects of stiffeners, resulting in highly conservative predictions for CFST and CFDT columns [23-25]

Research specifically addressing the behavior of stiffened CFDST and CFDT columns remains limited, with most studies focusing on a single stiffener type without comprehensive comparisons [26]. Earlier work on stiffened hybrid CFDT columns (using FRP for the outer tube) concluded that stiffening the inner tube is preferable for preventing local buckling and that a greater number of thin ribs performs better than a few thick ribs, sometimes increasing axial load capacity by over 50% [27-29]. Zeng et al. [30] examined the seismic performance of similar stiffened columns, concluding that increasing the number of ribs enhances energy dissipation and seismic performance. Other work confirmed the viability of specific design models for FRP-replaced external steel tubes in CFDST columns as proposed by Zeng et al. [31] and Yu et al. [32] , others introduced novel stiffener types, such as stirrups welded to both tubes, which offered optimal confinement at a specific ratio Ding et al. [33]

Studies on stiffened cold-formed double steel tube columns have also proposed new design formulas to correct the underestimation of load capacity by current codes, showing enhancements in both ultimate load capacity and ductility [34-37]

Wang et al. [38] and Ghannam and Metwally [39] demonstrated that T-stiffeners could increase the axial load capacity of circular CFDT columns by more than 15%. Further research confirmed that stiffening the outer tube increases the ductility and energy dissipation of CFDST columns Wang et al. [40] and that welded reinforcement bars enhance capacity, stiffness, and ductility, with inner tube stiffening providing the greatest enhancement. Hasan and Ekmekyapar [41]

Finally, T-stiffeners were found to improve the fire resistance of circular CFDST columns more effectively than rib stiffeners, yielding up to a 70% increase in fire resistance Shekastehband et al. [42]

It is anticipated that the addition of stiffeners will yield a more significant enhancement in the performance and load capacity of square CFDT columns compared to their circular counterparts. This expectation is based on the fact that circular tubes provide inherent confinement to the concrete due to the hoop tensile stress generated by the concrete's lateral expansion, a phenomenon largely absent in square columns, which are more susceptible to local buckling and confine the concrete only at the rounded corners [43-47].

While numerous studies have been conducted on stiffened CFST columns [20]; research focusing on stiffened CFDST and CFDT columns is scarce. The novelty of this study lies in addressing this critical research gap and developing simplified design guidelines for square CFDT column. This paper continues the second part of the research previously published by Ghannam and Metwally [39] which investigated the behavior of stiffened circular CFDT columns. While this paper focuses on the square cross-section, , also this study directly compare the performance of three distinct stiffener profiles (rectangular, inclined and tie stiffener) on the square CFDT columns under axila load. This comparison provides essential, previously unavailable design guidelines.

The objectives of this paper are achieved numerically using a Finite Element (FE) model developed in the ABAQUS program [48]. The FE model is verified against test results from [38], and subsequently employed to conduct a parametric analysis investigating the effect of various parameters on the behavior of stiffened square CFDT columns, which show the significant effect of tie stiffener in improves the performance of CFDT column compared to other studied stiffener types in this paper (Rectangular and incline stiffeners). Tie stiffeners can increase CFDT column ultimate strength by 15 %. Finally, a simplified analytical model is proposed to accurately predict the axial load capacity for these specific column types.

2. Finite element model

2.1. Description

2.1.1. Material models

Elastic-plastic stress-strain behaviour is used for square tubes, and multi-linear hardening is used for circular inner steel tubes similar to Tao et al. [49]. Concrete material is modelled using concrete-damaged plasticity [48]. The plasticity parameters are calculated as adopted by Tao et al. [49]. Ultimate tensile strength and corresponding fracture energy are used to simulate the tensile behaviour of concrete using ultimate tensile behaviour equal to 10% of compressive strength as proposed by Tao et al. [49],.

2.1.2. Interactions and constrains

Interaction between concrete and steel tubes is simulated by using surface-to-surface contact. The value of Coulomb friction is taken as 0.6. Tie constraints were used to model the contact between steel tubes and stiffeners which insure full attachment between both parts. Tie also are used between concrete and stiffeners, Ghannam and Metwally [39] compare between modeling the interaction between concrete and stiffeners as tie and as contact interaction and found that both gives similar results as stiffeners is completely embedded in the concrete.

2.1.3. Boundary conditions and element divisions

Solid element (C3D8R) was used to model concrete, while shell element (S4R) was used to model steel tubes and stiffeners. The top of the column was coupled with a reference point (using coupling constraint), where this point controls the column's top displacement and rotation. To save computational time and gain the benefits of model symmetry, a quarter model is used using half-length and half-section. The number of elements was determined after performing a sensitivity analysis.

The corner of the outer steel tube of the CFDT square column was modelled once as a sharp edge and another time as a curved edge. From Fig. 1, it can be seen that there was no significant effect. So, a sharp edge was chosen in order to simplify the model geometry. The column width is divided in to 12 elements, while the element size in the longitudinal direction is twice that within the cross-section [39]. Mesh size and division were obtained based on mesh sensitivity analysis. Several number of element divisions were used to show the optimum number of element that provide closer agreement with test result and also saving computational time. It was found that using smaller number of division provides less accuracy, using 12 elements division provide closer agreement to the test result without increasing the computational time, increasing number of elements more than this has minor effect on model accuracy.

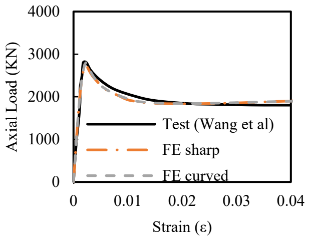

Fig. 1 Effect of square section corner shape

2.1.4. Initial imperfection and residual stress

Initial imperfection was included to the FE model through a separate buckling analysis where the first buckling mode with an amplitude equal to column length/1000, was implemented in the stress analysis as an initial state of the columns.

Previous researchs [50-53] shows that effect of residual stress can be ignored as they have minor effect on initial stiffness, ultimate load an overall performance. [52] shows that this is due to the presence of concrete which take part in carrying large portion of the columns load capacity.

2.2. Verification of the FE model

Due to limited research on stiffened square CFDT columns, the FE model was verified against test results that were performed by [38] for stiffened square double tube columns using four welded lipped angle (23 mm lip) for the outer steel tube and circular tube for inner steel, Also, [19, 54] were used for stiffened square CFST columns. Details of the specimens are presented in Table 1. The first column is the specimen ID and the references between square brackets; other column headings contain Do and to are the column's outer tube width and thickness, respectively, Di and ti are the column's inner tube width and thickness, respectively. fyo, fco', fyi, and fci are the outer steel tube yield strength, outer concrete ring cylinder compressive strength, inner steel tube yield strength and inner concrete core cylinder compressive strength, respectively. Specimens that do not have Di and ti and fyi, and fci' are CFST columns. Nu,test and Nu,FE are the ultimate loads obtained from the test and finite element (FE) model. L is the column's total length. The last column in the table contain cross-section shapes snd stiffeners.

Table 1
Test specimens details used in verification

Speci-mens [ref]	Do (mm)	to (mm)	Di (mm)	Ti (mm)	L (mm)	f_{yo} MPa	f_{co}' MPa	f_{yi} MPa	f_{ci}' MPa	Nu (KN) Test	Nu (KN) FE	Cross-section
SDS1-40a [38]	200	2.01	136.5	1.94	600	230	42.1	492.1	42.1	2450	2414.1	
SDS1-70a [38]	200	2.01	136.5	1.94	600	230	42.1	492.1	69.8	2806	2740.4	
SDS2-40a [38]	200	2.01	114.6	3.93	600	230	42.1	377.1	42.1	2463	2615	
SDS2-70a [38]	200	2.01	114.6	3.93	600	230	42.1	377.1	69.8	2765	2788.8	
SDS3-40a [38]	200	2.01	140.1	3.78	600	230	42.1	322.4	42.1	2505	2588.4	
SDS3-70a [38]	200	2.01	140.1	3.78	600	230	42.1	322.4	69.8	3100	2899.8	
SS-040-050~3 [54]	200	5	-	-	600	265.8	27.15	-	-	2728	2093.2	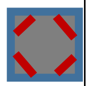
SS-040-050~4 [54]	200	5	-	-	600	265.8	27.15	-	-	2903	2090.2	
SS-040-100~4 [54]	200	5	-	-	600	265.8	27.15	-	-	2463	2089.2	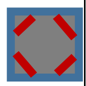
SS-070-093~2 [54]	280	4	-	-	840	272.6	30.49	-	-	3744	3507.8	
SS-070-093-3 [54]	280	4	-	-	840	272.6	30.49	-	-	3855	3652.6	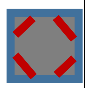

Speci-mens [ref]	Do (mm)	to (mm)	Di (mm)	Ti (mm)	L (mm)	f_{yo} MPa	f_{co}' MPa	f_{yi} MPa	f_{ci}' MPa	Nu (KN) Test	Nu (KN) FE	Cross-section
SS-070-187-3 [54]	280	4	-	-	840	272.6	29.18	-	-	3457	3381.2	
SCFT 1-1 [19]	200	2.5	-	-	1190	270	49.3	-	-	2640	2398.8	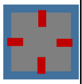
SCFT 2-1 [19]	200	2.5	-	-	2340	270	49.3	-	-	2455	2381.9	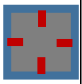

Fig. 2 shows the comparison the test results and FE model in accordance to axial load and axial strain curve. It can be seen that there is a reasonable correlation between the test results and FE model results. The average value for axial load capacity obtained from the test result to that obtained from the FE model is 1.08 with COV = 0.12.

Fig. 3 shows the comparison between the failure mode obtained from the test and the FE model. All specimens fail due to local buckling of the steel tube. As can be seen from Fig. 3, the FE model tracks a similar failure mode as the test specimens.

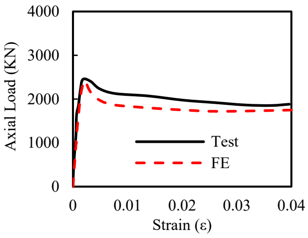

(a) SDS1-40 [38]

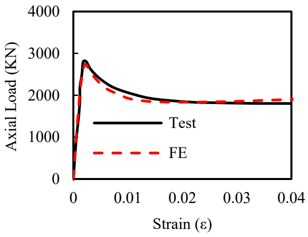

(b) SDS1-70 [38]

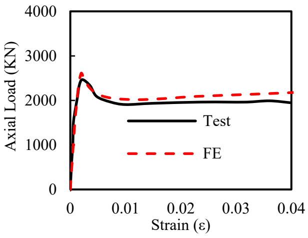

(c) SDS2-40 [38]

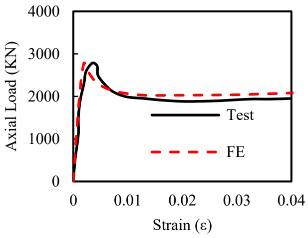

(d) SDS2-70 [38]

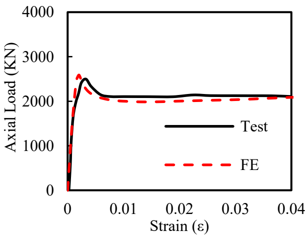

(e) SDS3-40 [38]

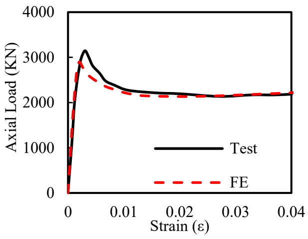

(f) SDS3-70 [38]

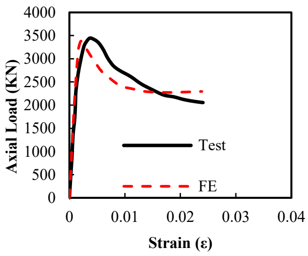

(g) SS-070-187 (3) [50]

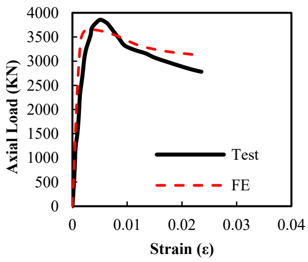

(h) SS-070-93 (3) [50]

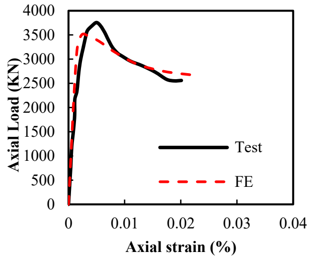

(i) SS-070-93 (2) [50]

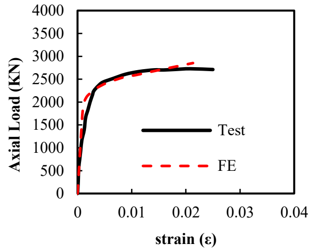

(j) SS-040-50 (3) [50]

Fig. 2 Comparison between test results and FE model

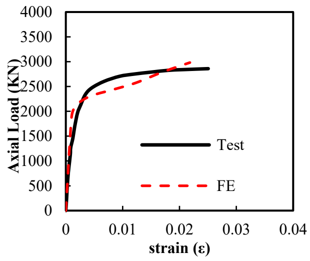

(k) SS-040-50 (4) [50]

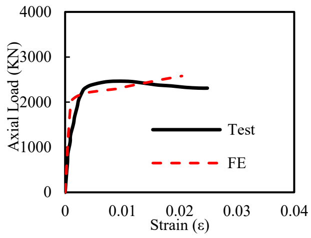

(l) SS-040-100 (3) [50]

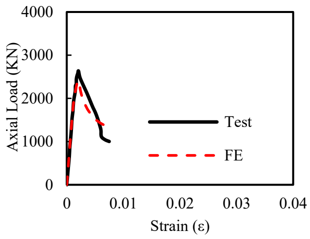

(m) SCFT1-1 [19]

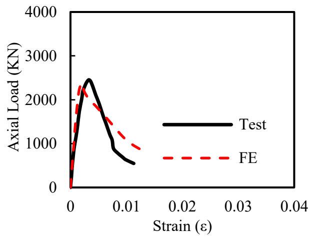

(n) SCFT2-1 [19]

Fig. 2 Comparison between test results and FE model (continue)

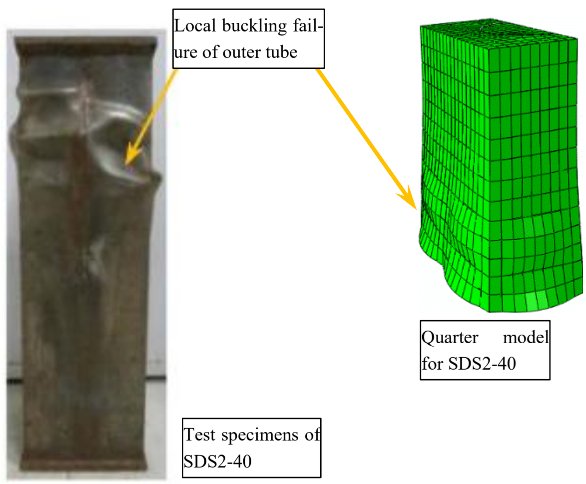

Fig. 3 Failure mode comparison between test specimens SDS2-40 and FE model

3. Analysis of different types of stiffeners

Three types of stiffeners, such as longitudinal rectangular plate (R), inclined plate (Inclined) and ties as shown in Fig. 4, are investigated in this paper. Their effects are compared with the control model with an outer diameter of 500 mm and a length of 8000 mm for slender columns, 1500 mm for stub columns, and 250 mm outer dimension of the inner tube. The D/t ratio is kept constant at 100.

The dimension of the rectangular stiffener was determined according to the research performed by Tao *et al.* [52], with stiffener length equal to 81 and 40.5 mm for outer and inner tube respectively, thickness for stiffener was kept the same as the steel tube (5 and 2.5 mm for outer and inner tube respectively) .

For Inclined stiffeners the inclined length is equal to 464 and 232 mm attached to outer and inner tube respectively with 5 and 2.5 mm thickness attached to outer and inner tube respectively. No of inclined stiffener per meter is 3 for the outer tube and 6 for the inner tube.

The dimeter of Ties was 18 and 12 mm for outer and inner tube respectively and length of 230 and 115 for outer and inner tube respectively with keeping the number equal to 7 for both tubes.

Tie and inclined stiffeners were determined to maintain the same weight as the rectangular stiffener. This is to ensure that the weight and cost of different stiffening techniques are nearly the same.

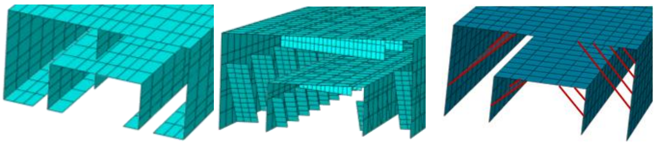

(a) Rectangular (b) Inclined (c) Tie

Fig. 4 Different types of stiffeners used in this study (half column section in abaqus)

It can be seen from Fig. 5 that the three types of stiffeners increase the ultimate load capacity for the columns for slender and stub columns. From the failure mode shown in Fig. 6a, it can be shown the half wavelength of the buckling of the unstiffened column is equal to the column width. For inclined stiffeners (Fig. 6b), the wavelength takes an inclined shape parallel to the inclined stiffeners. From Fig. 6c, half wavelength is equal to half column width as single rectangular stiffeners are placed in the middle of the column cross section, which helped in reducing the wavelength. In case ot Ties half wavelength for buckling is equal to one-third of the column width at the fixation point of ties. This explains the increased ultimate force in stiffened columns compared to unstiffened ones. Tie stiffeners provide less half wave length compared to other stiffners type which will delay local buckling of outer esteel tube providing more ultimate strength using Tie stiffeners.

Fig. 7 shows the contact pressure distribution over the outer and inner concrete core. It can be seen that the pressure in the unstiffened column is concentrated at corners with nearly zero at the middle, which explains the failure mode presented in Fig. 6a. Although contact pressure in stiffened columns has a lower maximum value than that of unstiffened columns, the pressure is distributed over a more concrete surface area than the unstiffened columns. In the case of inclined stiffened, pressure takes an inclined shape similar to the inclined stiffeners.

It can also be seen from Fig. 7 that contact pressure in rectangular stiffeners is concentrated at corners and at the location of rectangular stiffeners. A similar situation is presented in tie stiffeners where maximum pressure is located at corners and at the connection of ties with steel tubes. As a result of more contact pressure in Tie stiffened columns, more confinement pressure is provided to the concrete core (co mpared to other stiffeners) , which helps in increasing the load capacity of the columns, thanks to the tensile force formed in the ties due to the latteral expansion of concrete formed from axial froce. The formed tensile force will prevent outward buckling of steel tube and providing more contact between steel tube and concrete increasing interaction between both material. From the previous discussion, it can be concluded that the improvement in ultimate strength for stiffened columns over unstiffened columns is due to the reduction in steel tube buckling and concrete confinement.

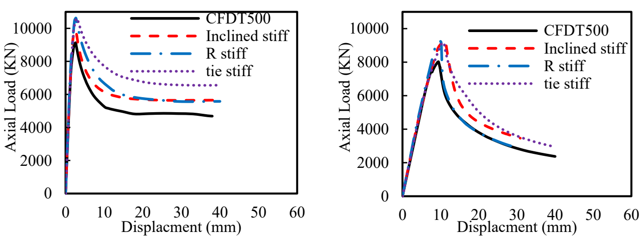

(a) Stub (b) Slender

Fig. 5 Effect of stiffeners on axial displacement curve

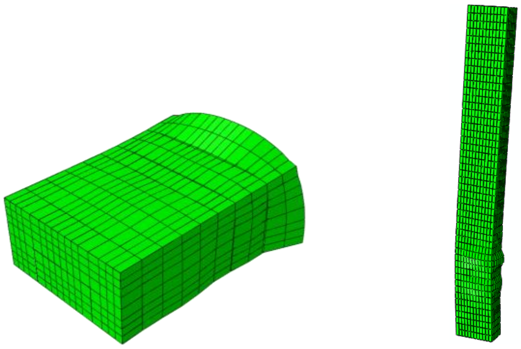

Stub columns Slender columns

a) un-stiffened columns

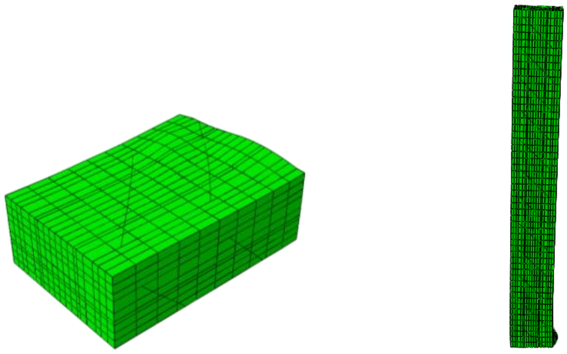

Stub columns Slender columns

b) Inclined stiffeners

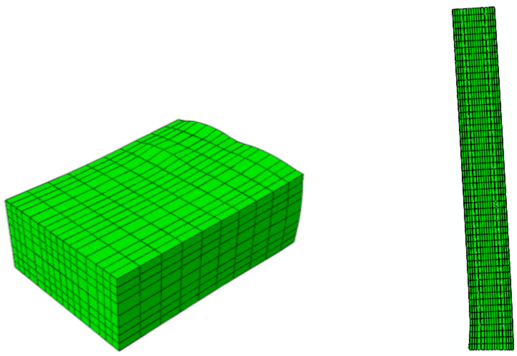

Stub columns Slender columns

c) Rectangular stiffeners

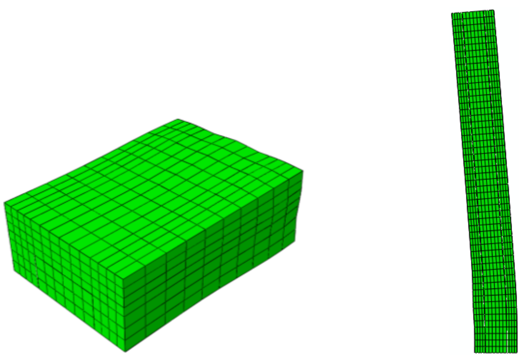

Stub columns slender columns

d) tie stiffeners

Fig. 6 Failure mode for different types of stiffeners

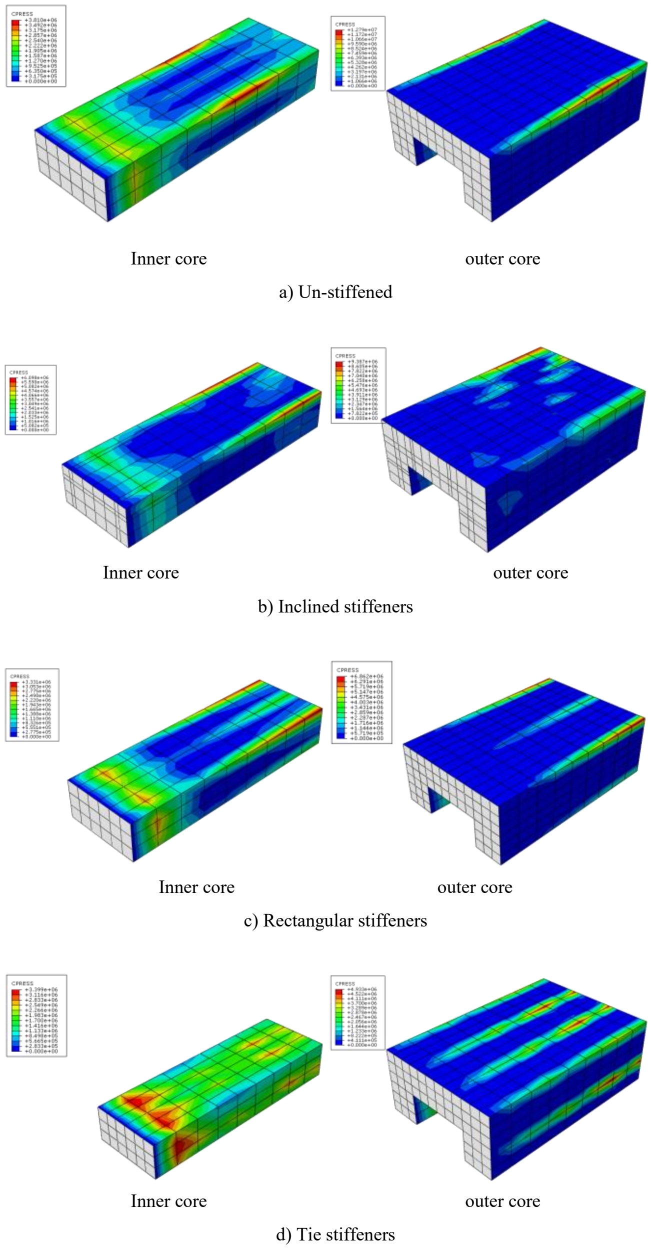

Fig. 7 Contact pressure in different stiffening profile

4. Parametric studies

This section presents a parametric study based on the finite element results. The analysis is performed on unstiffened and different stiffened column profiles (inclined, Rectangular and Tie stiffeners)

4.1. Effect of outer tube width to thickness ratio (Do/to)

Fig. 8 shows the effect of the outer tube width-to-thickness ratio on the ultimate load capacity and column behaviour. It can be seen that column strength and initial stiffness during the elastic zone increase significantly by increasing outer tube thickness as concrete is replaced with steel material since the outer tube dimension is kept constant, besides it decrease the local buckling of the outer tube.

4.2. Effect of inner tube width to thickness ratio (Di/ti)

The effect of the inner tube width-to-thickness ratio on column behaviour is shown in Fig. 9. It is found that the inner tube thickness is less significant than the outer tube thickness due to the larger steel area increase in the outer tube compared to the inner tube. Besides, the inner tube is more restrained against buckling compared to the outer tube as concrete in surrounds the inner tube from the inner and outer sides of the tube, unlike the outer tube where concrete is placed only from the inner side of the tube, providing less restraint to buckling. Increasing the outer tube thickness will have more effect in reducing tube buckling compared to the inner tube.

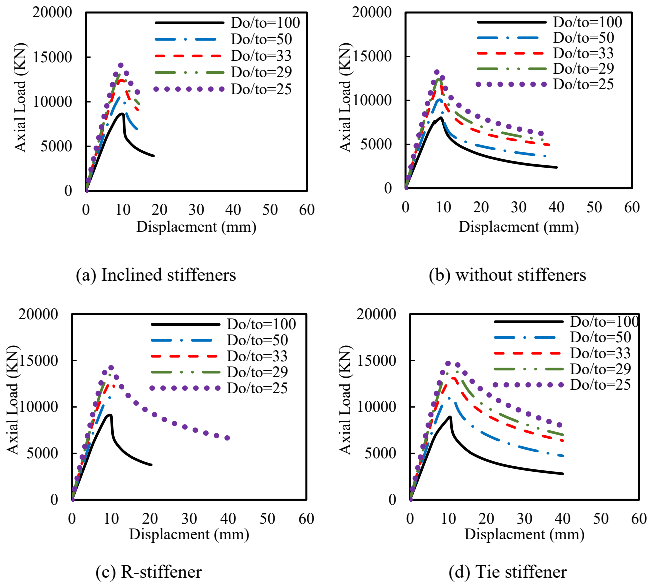

Fig. 8 Effect of outer tube width to thickness ratio (Do/to)

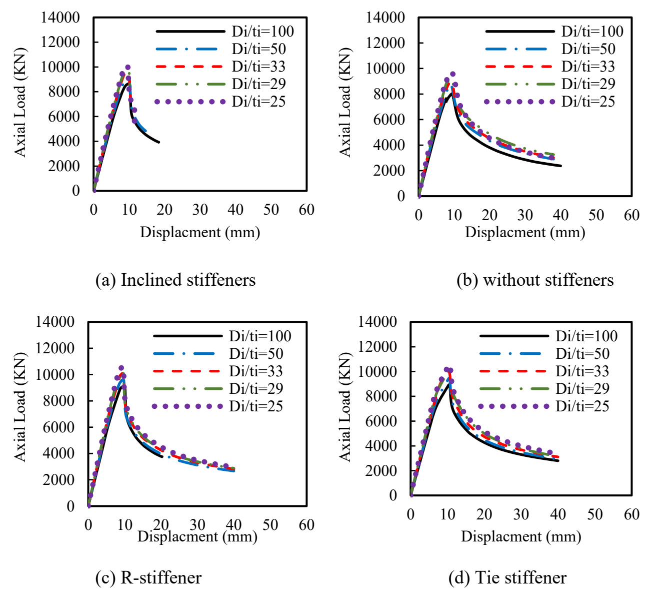

Fig. 9 Effect of inner tube width to thickness ratio (Di/ti)

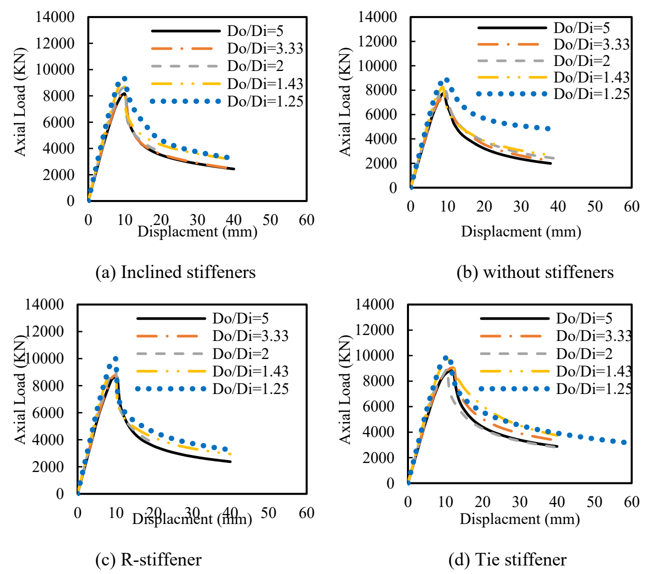

Fig. 10 Effect outer to inner tube width (Do/Di)

4.3. Effect outer to inner tube width (Do/Di)

In this case, the inner tube width is changed, and the outer tube width is kept constant. The effect of outer-to-inner tube diameter on ultimate column strength was not significant compared to the effect of Do/to ratio. The slender columns studied in this paper fail mainly due to a combination of outer tube local buckling and overall global buckling, as indicated previously in Fig. 6. Increasing the inner tube width will have minor effect in increasing column flexural stiffness (EI/L). This case is different from concrete-filled double skin tube columns where inner core is void so in this case increasing and decreasing column width will have a significant effect on column flexural stiffness.

4.4. Effect of concrete compressive strength (fc') and steel tube yield strength (fy)

Concrete strength has a significant effect on the ultimate strength of the CFDT column as the concrete area takes up a large portion of the column cross-section. So, increasing concrete strength will result directly in a significant increase in the column's ultimate strength. This is indicated in Fig. 11. Fig. 12 shows that steel tube yield strength significantly affects column ultimate strength, similar to the case of concrete compressive strength. Increasing yield strength leads to increasing column ultimate strength as a direct result of increasing axial load capacity of steel inner and outer tube. Besides, increasing steel yield strength will help increase the confinement of concrete provided by steel tubes. It can be seen that the effect of concrete strength is more effective compared to increasing column ultimate strength as the cross-sectional area of concrete is larger than that of steel tube.

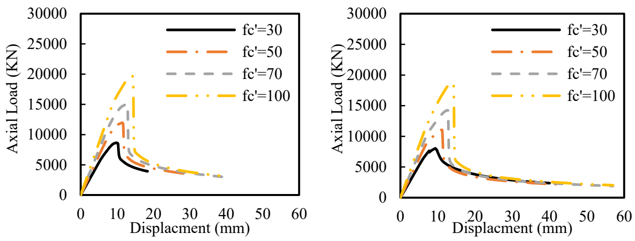

(a) Inclined stiffeners (b) without stiffeners

(c) R-stiffener (d) Tie stiffener

Fig. 11 Effect of concrete compressive strength (fc')

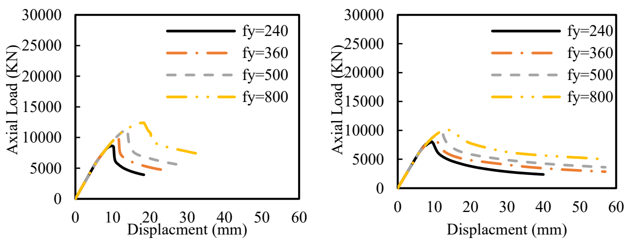

(a) Inclined stiffeners (b) without stiffeners

(c) R-stiffener (d) Tie stiffener

Fig. 12 Effect of steel tube yield strength (*fy*)

4.5. Effect of Slenderness ratio (λ)

Fig. 13 shows the effect of the column slenderness ratio on the column behaviour. It can be concluded that column slenderness has a negative significant effect on column ultimate strength. This is due to the reduction in the flexural stiffness of the column due to the increase in column length and slenderness. Besides, increasing column length will lead to an increase in the second-order effect provided by imperfection, which is taken equal to L/1000.

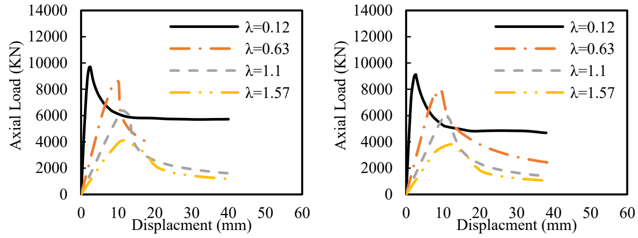

(a) Inclined stiffeners (b) without stiffeners

(c) R-stiffener (d) Tie stiffener

Fig. 13 Effect of Slenderness ratio (λ)

4.6. Effect of different stiffener profiles

From Figs. 8 to 13, it can be concluded that inclined, rectangular and tie stiffeners provided an increase in column ultimate strength with an average value (ultimate strength with stiffeners/ ultimate strength with no stiffeners) of 1.08, 1.14 and 1.15, respectively. This shows that rectangular and tie stiffeners increase ultimate strength the most.

This can be attributed to the profile of each stiffener. In the case of rectangular stiffeners, the local buckling occurred over half the column width due to the presence of stiffeners at the middle of the column width. While in tie stiffeners, buckling occurred at one-third of the tube width at the location of the tie fixation point with the tube, which will provide more contact area with concrete leading to more confinement, as presented in Fig. 7. Meanwhile, in inclined stiffeners, the local buckling occurs at the whole width of the inclined line parallel to the inclined stiffeners, providing the least confinement to concrete.

The ductility of each type of profile was determined according to the ductility index as presented by Tao *et al.* [52], which stated that the ductility index (DI) is equal to $\varepsilon_{(85\%)}/\varepsilon_y$ where $\varepsilon_{(85\%)}$ is the strain when the load fail to 85% of the ultimate load and $\varepsilon_y = \varepsilon_{(75\%)}/0.75$ where $\varepsilon_{(75\%)}$ is the ultimate strain when the load become 75 % of the ultimate load and before it reaches it. The average value of DI in the case of inclined, rectangular and Tie stiffeners is 1.34, 1.32 and 1.46, respectively. This shows that tie stiffeners provide more ductility compared to other stiffener types, owing to the delay in outer tube buckling due to the restraints provided by tie stiffeners to the steel tubes, as shown in Figs. 6 and 7. Further investigation is performed on tie stiffener as it provides the most increase in ultimate load value.

In Fig. 14, two parameters were investigated for tie stiffeners. Fig. 14a studied the effect of tie's diameter on colum behaviour. It was found that the diameter has an insignificant effect on ultimate load value while it provides a significant effect on post-ultimate load behaviour. Increasing ties diameter decreases the post failure deformation of the columns as increasing the tie diameter helps in increasing its axial stiffness, which will provide more restraint to the steel tube against buckling. However, it cannot eliminate buckling. Spacing between ties was investigated in Fig. 14b. It is found that decreasing tie's spacing will help in increasing column ultimate load and improve the post failure behaviour as a result of decreasing the steel tube buckling length in longitudinal direction.

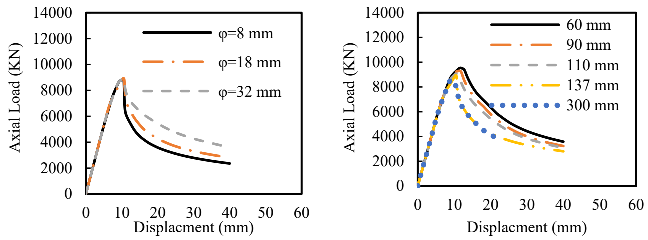

(a) Diameter of tie stiffeners (b) spacing between Tie stiffeners

Fig. 14 Parameters for Tie stiffeners

5. Proposed analytical model

In this section a simplified analytical model based on Eurocode 4 [55] is proposed to predict the ultimate strength of stiffened CFDT column using tie stiffeners. The design of composite columns in Eurocode 4 is applied for CFST column. However, it can be modified to fit CFDT columns as follows:

$$N_{\mathrm{pl,Rd}} = A_{\mathrm{so}} \times f_{\mathrm{yo}} + A_{\mathrm{si}} \times f_{\mathrm{yi}} + A_{\mathrm{co}} \times f'_{\mathrm{co}} + A_{\mathrm{ci}} \times f'_{\mathrm{ci}} \quad (1)$$

Where $N_{\mathrm{pl,Rd}}$ is the load-carrying capacity for the column based on cross-section capacity; A_{so} and A_{si} is the cross-sectional area for the outer and inner steel tube, respectively; $f_{\mathrm{so,y}}$ and $f_{\mathrm{si,y}}$ is the yield strength for the inner and outer steel tube, respectively; A_{co} and A_{ci} is the cross-sectional area of the outer concrete ring and inner concrete core, respectively ; f'_{co} and f_{ci}' is the compressive strength of the outer concrete ring and inner concrete core, respectively.

$$N_{\mathrm{b,Rd}} = \chi N_{\mathrm{pl,Rd}} \,, \quad (2)$$

Where $N_{\mathrm{b,Rd}}$ is the buckling load capacity for columns.

$$X = \frac{1}{\phi + \sqrt{\phi^2 - \lambda^2}} \quad (3)$$

$\phi = 0.5\,(1 + \alpha\,(\lambda - 0.2) + \lambda^{2.4})$, α is the type of buckling curve used in calculation based on section type and equal to 0.21 if reinforcement in the cross-section is less than 3%. 0.34 is used if the reinforcement ratio is more than 3% can be used. In the CFDT columns, the area of the inner steel tube is used as an equivalent to the reinforcement ratio.

$$\lambda = \sqrt{N_{\mathrm{pl,Rd}} / N_{\mathrm{cr}}}$$

$$N_{\mathrm{cr}} = \pi^2 \,(E\,I)_{\mathrm{eff}} / l_b^2 \quad (4)$$

$$EI_{\mathrm{eff}} = E_{\mathrm{so}} \times I_{\mathrm{so}} + E_{\mathrm{si}} \times I_{\mathrm{si}} + 0.6\left(E_{\mathrm{co}} \times I_{\mathrm{co}} + E_{\mathrm{ci}} \times I_{\mathrm{ci}} \right) \quad (5)$$

E_{so} and E_{si} are the modulus of elasticity for outer and inner steel tubes, E_{co} and E_{ci} is the modulus of elasticity for outer and inner concrete, respectively concrete, I_{so} and I_{si} are the inertia for outer and inner steel tube, respectively. While I_{co} and I_{ci} are the inertia of outer and inner concrete respectively.

The ultimate load obtained from Eurocode 4 , AISC [56] and AIJ [57] are evaluated against the FE model ultimate load. The result is presented in Fig. 15 and Table 2. It can be seen that Eurocode 4, AISC [56] and AIJ [57] gives conservative results compared to the FE model results, with Eurocode closer to FE results, which mostly lead to an uneconomic design. This conclusion is similar to that obtained from previous researchers [23-25].

A new model is proposed, which predicts the ultimate load capacity of stiffened square CFDT columns using tie stiffeners. The proposed model is based on the Eurocode 4 model for unstiffened CFDT columns, as stated below:

$$N_{\mathrm{pl,Rd}} = \beta_{so} \times A_{\mathrm{so}} \times f_{\mathrm{so,y}} + \beta_{si} \times A_{\mathrm{si}} \times f_{\mathrm{si,y}} + \beta_{co} \times A_{\mathrm{co}} \times f'_{\mathrm{co}} + \beta_{ci} \times A_{\mathrm{ci}} \times f'_{\mathrm{ci}} \quad (6)$$

Where: β_{so}, β_{si}, β_{co}, β_{ci} are the correction factors for outer steel tube, inner steel tube, outer concrete ring and inner concrete core, respectively. These factors consider the delay in local buckling of steel tube and concrete confinement formed due to the presence of tie stiffeners. The correction factors are obtained through nonlinear regression analysis as follows:

$$\beta_{so} = -3.674E^{-4}(b/t)^2 + 0.035(b/t) - 0.0107(S/t) - 3.370X^2 + 3.452X + 7.272E^{-4}\xi^{-2.202} - 0.0667 \quad (7)$$

$$\beta_{co} = 0.00218(b/to) + 4.803E^{-4}(S/t) + 0.0218X^2 - 0.265X + 18.188\xi^{0.00366} - 16.924 \quad (8)$$

$$\beta_{si} = 0.00179(b/to) - 2.299E^{-4}(S/t) - 0.538X^2 + 0.449X + 0.209(fyi/240) + 0.737 \quad (9)$$

$$\beta_{ci} = 0.0117(b/to) + 1.3515E^{-4}(S/t)^2 - 0.0112(S/t) - 0.317X^2 - 0.167X - 0.287\xi^2 + 0.627\xi + 0.986 \quad (10)$$

Where b is the longest unsupported length of outer steel tube width in horizontal direction and it is equal to tube outer width /3 if the ties support the tube at two intermediate points equally spaced, t is the thickness of outer steel tube and "S" is the spacing between tie in longitudinal direction of the columns X is the ratio between outer and concrete core width and equal Di/(Do-2to), fyi is the inner steel tube yield strength (Mpa) and ξ is confinement coefficient and equal to:

$$\frac{A_{so} \cdot f_{yo}}{A_{co} \cdot f'_{co}} \,.$$

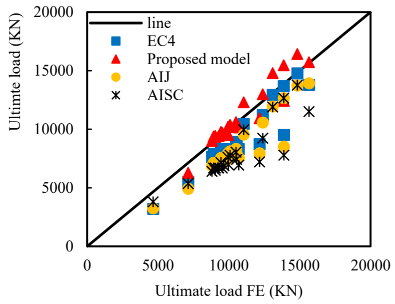

Fig. 15 Evaluation for Eurocode and proposed model

Table 2
Comparison between EC4 and proposed model

	N_ED (EC4)/N_FE	N_ED (AIJ)/N_FE	N_ED (AISC)/N_FE	N_ED(Pro-posed model)/N_FE
Avg	0.846	0.79	0.75	0.999
COV	0.095	0.104	0.118	0.086

The relation between β_{so} , β_{co} , β_{si} and β_{ci} and other significant parameters, such as unsupported steel tube horizontal width to thickness ratio, stiffener longitudinal spacing to tube thickness ratio, outer tube width to inner concrete width ratio, steel tube yield strength, and confinement ratio, are presented in Figs. 16 to 19. In Figs. 16 to 19, the terms $N_{\mathrm{so\_no\ stiffener}}$, $N_{\mathrm{co\_no\ stiffener}}$, $N_{\mathrm{si\_no\ stiffener}}$ and $N_{\mathrm{ci\_no\ stiffener}}$ are the axial load capacity for outer steel tube, outer concrete ring, inner steel tube and inner concrete core without the effect of any stiffeners respectively. At the same time, N_{so_tie}, $N_{\mathrm{co\_tie}}$, $N_{\mathrm{si\_tie}}$ and $N_{\mathrm{ci\_tie}}$ are the axial load capacity for the outer steel tube, outer concrete ring, inner steel tube and inner concrete core using tie stiffener, respectively. The horizontal axis in these curves represents different parameters effect including unsupported steel tube horizontal width to thickness ratio (b/t), stiffener longitudinal spacing to tube thickness ratio (*S/t)*, outer tube width to inner concrete width ratio (*X),* steel tube yield strength (f_{yi}/240) and confinement ratio (ξ).

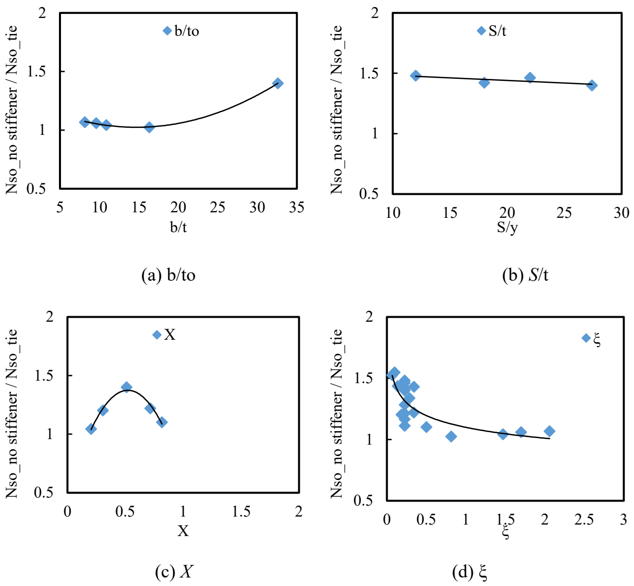

Fig. 16 Effect of different parameters on βso

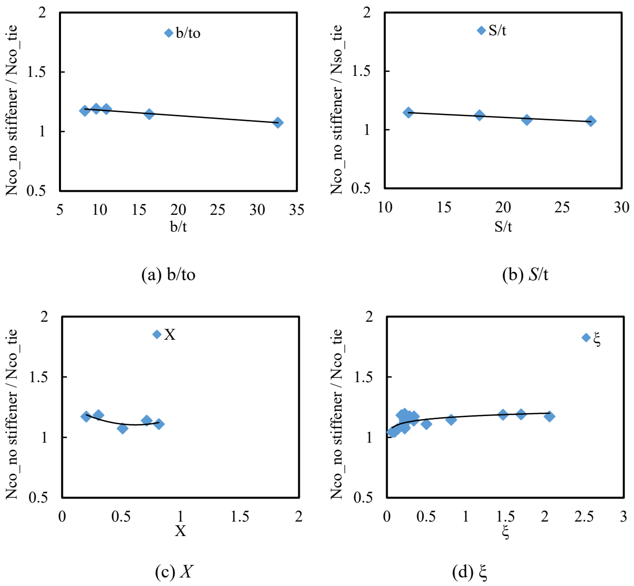

Fig. 17 Effect of different parameters on βco

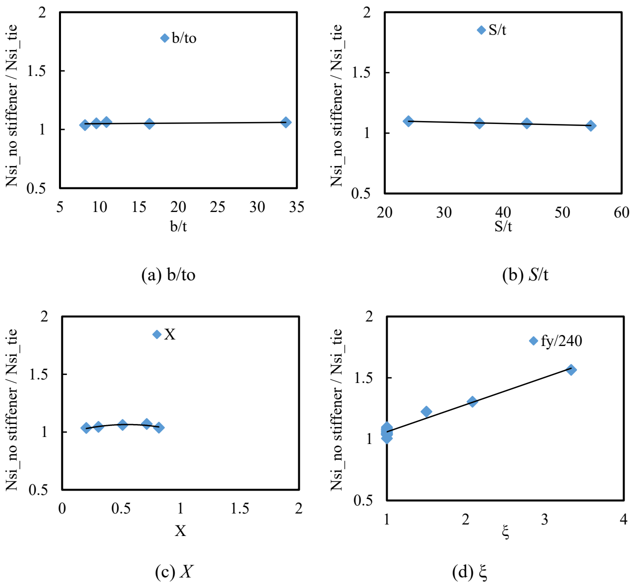

Fig. 18 Effect of different parameters on βsi

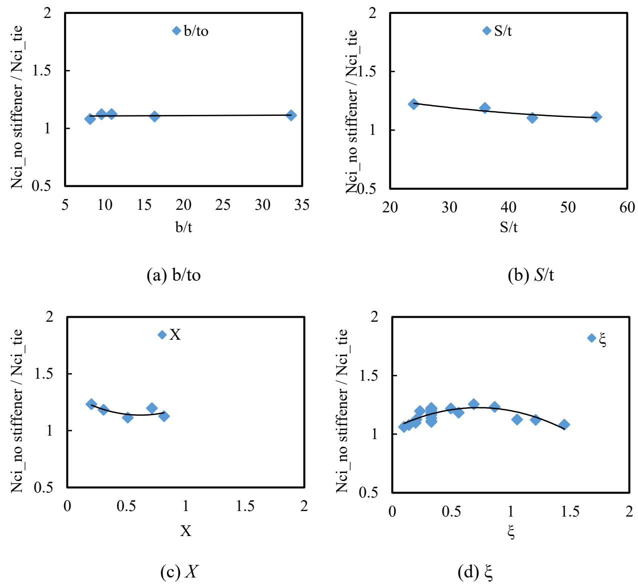

Fig. 19 Effect of different parameters on βci

The rest of the steps to calculate $N_{b,Rd}$ is similar to Eurocode 4. However, α is equal to 0.13. A comparison between the Eurocode buckling curve and the proposed buckling curve is shown in Fig. 20. The y-axis represents column slenderness (λ), and the x-axis represents the slenderness reduction factor (χ). N_FE represent the axial load of slender columns obtained from finite element (FE), while, Npl_Rd is the plastic resistance for cross-section as indicated in Equation (6), taking into account the effect of tie stiffener. Fig. 15 and Table 2 show the comparison between the proposed model and Eurocode 4, AISC and AIJ model. It can be found that the proposed mode gives better results compared to other standerds in terms of average value (avg) and coefficient of variance (COV) as indicated in Table 2.

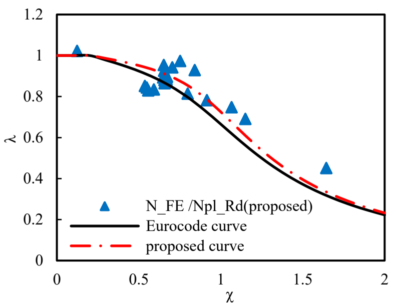

Fig. 20 Comparison between euro code buckling curve and proposed curve

6. Conclusions

This paper presented a numerical study on the behaviour of stiffened square CFDT columns. Three types of stiffeners were studied: inclined, rectangular and Tie stiffeners. A verified FE model was developed in order to give a better understanding for this type of column. The verified FE model was used in providing a parametric study and proposing a simplified analytical model. The following conclusion can be drawn based on the parametric study performed based on the FE model:

- The outer tube width-to-thickness ratio has a significant effect on ultimate strength and initial stiffness. Specifically, a reduction in the outer tube width-to-thickness ratio yields a substantial increase in the column's ultimate strength, dominating the effects of both the inner tube width-to-thickness ratio and the outer-to-inner tube width ratio. Decreasing outer tube width-to-thickness ratio will lead to a decrease in outer tube local buckling and as the outer dimension is kept constant decreasing outer tube width-to-thickness ratio leads to a decrease in concrete area and an increase in steel area, which will increase the capacity of the columns.
- Both the inner tube width-to-thickness ratio and the outer tube width-to-inner width ratio exhibit an inverse relationship with the ultimate compressive strength of the column.
- The use of Tie stiffeners provides a superior performance profile under axial loading, significantly enhancing both the ultimate load capacity and the ductility of the CFDT column. The ultimate load was observed to

increase by over 15% when incorporating Tie stiffeners compared to other configurations. This is due to the lower value of half wave length of the steel tube buckling compared to other stiffeners configurations and the higher confinement provided by the ties stiffeners to concrete thanks to the tensile fore formed in the ties preventing outward buckling of steel tube and providing more contact between steel tube and concrete

- The ultimate load of the CFDT column is inversely proportional to the longitudinal spacing of the Tie stiffeners; closer spacing leads to a higher ultimate capacity
- Increasing the diameter of the Tie stiffeners does not influence the column's ultimate strength; however, it demonstrably improves the structural performance during the post-ultimate load stage (enhancing residual capacity and stability).
- A simplified analytical model was successfully proposed to estimate the ultimate load capacity of CFDT columns utilizing Tie stiffeners. This model, which is fundamentally based on the principles of Eurocode 4, demonstrates strong agreement with the results generated by the detailed FE model.

Data availability

No data was used for the research described in the article

List of abbrevitaions

Symbol	Definition
Aci	the cross-sectional area of inner concrete core
Aco	the cross-sectional area of the outer concrete ring
Asi	the cross-sectional area for the inner steel tube
Aso	the cross-sectional area for the outer steel tube
b	longest unsupported length of outer steel tube width in horizontal direction
Di	column's inner tube width
Do	column's outer tube width
Eci	modulus of elasticity for inner concrete
Eco	modulus of elasticity for outer concrete
Esi	modulus of elasticity for inner steel tubes
Eso	modulus of elasticity for outer steel tubes
fci	inner concrete core cylinder compressive strength
fco’	outer concrete ring cylinder compressive strength
fyi	inner steel tube yield strength
fyo	outer steel tube yield strength
Ici	inertia of inner concrete
Ico	inertia of outer concrete
Isi	inertia for inner steel tube
Iso	inertia for outer steel tube
L	column's total length
Nb,Rd	the buckling load capacity for column
Nci_no stiffener	axial load capacity inner concrete core without using any stiffeners
Nci_tie	axial load capacity inner concrete core using tie stiffener
Nco_no stiffener	axial load capacity for outer concrete ring without using any stiffeners
Nco_tie	axial load capacity for outer concrete ring using tie stiffener
Nsi_no stiffener	axial load capacity for inner steel tube without using any stiffeners
Nsi_tie	axial load capacity for inner steel tube using tie stiffener
Nso_no stiffener	axial load capacity for outer steel tube without using any stiffeners
Nso_tie	axial load capacity for outer steel tube using tie stiffener
Nu,FE	ultimate loads obtained from the Finite elemnt (FE) model
Nu,test	ultimate loads obtained from the test
S	the spacing between tie in longitudinal direction of the columns
ti	column's inner tube thickness
to	column's outer tube thickness
X	ratio between outer and concrete core width and equal Di/(Do-2to)
β_ci	correction factors for inner concrete core
β_co	correction factors for outer concrete ring
β_si	correction factors for inner steel tube
β_so	correction factors for outer steel tube
ξ	confinement coefficient
χ	slenderness reduction factor

References

[1] Romero ML, Espinos A, Portolés JM, Hospitaler A, Ibañez C. Slender double-tube ultra-high strength concrete-filled tubular columns under ambient temperature and fire. Engineering Structures. 2015;99:536-45.
[2] Tao Z, Han L-H, Zhao X-L. Behaviour of concrete-filled double skin (CHS inner and CHS outer) steel tubular stub columns and beam-columns. Journal of Constructional Steel Research. 2004;60:1129-58.
[3] Tao Z, Han L-H. Behaviour of concrete-filled double skin rectangular steel tubular beam–columns. Journal of Constructional Steel Research. 2006;62:631-46.
[4] Han L-H, Huang H, Tao Z, Zhao X-L. Concrete-filled double skin steel tubular (CFDST) beam–columns subjected to cyclic bending. Engineering Structures. 2006;28:1698-714.
[5] Mohan AP, S A. Non-Linear Analysis of Concrete Filled Double Skin Circular Steel Column. International Journal of Engineering Research & Technology (IJERT). 2016;5:204-6.
[6] Elchalakani M, Hassanein MF, Karrech A, Yang B. Experimental investigation of rubberised concrete-filled double skin square tubular columns under axial compression. Engineering Structures. 2018;171:730-46.
[7] Hassanein MF, Elchalakani M, Karrech A, Patel VI, Daher E. Finite element modelling of concrete-filled double-skin short compression members with CHS outer and SHS inner tubes. Marine Structures. 2018;61:85-99.
[8] Zhao X-L, Han L-H. Double skin composite construction. Progress in Structural Engineering and Materials. 2006;8:93-102.
[9] Huang H, Han L-H, Tao Z, Zhao X-L. Analytical behaviour of concrete-filled double skin steel tubular (CFDST) stub columns. Journal of Constructional Steel Research. 2010;66:542-55.
[10] Ekmekyapar T, Al-Eliwi BJM. Concrete filled double circular steel tube (CFDCST) stub columns. Engineering Structures. 2017;135:68-80.
[11] Jin K-Y, Zhou X-H, Wen H, Deng R, Li R-F, Wang Y-H. Compressive behaviour of stiffened thin-walled CFDST columns with large hollow ratio. Journal of Constructional Steel Research. 2023;205:107886.
[12] Li B-F, Wang X-T, Xie C-D, Yan X-F, Wang S. Compressive behaviour and design of tapered lightweight concrete-filled double-skin stiffened steel tubular short columns with large hollow ratio. Structures. 2024;64:106527.
[13] Cai J, He Z-Q. Axial load behavior of square CFT stub column with binding bars. Journal of Constructional Steel Research. 2006;62:472-83.
[14] Younes SM, Ramadan HM, Mourad SA. Stiffening of short small-size circular composite steel–concrete columns with shear connectors. Journal of Advanced Research. 2016;7:525-38.
[15] Lai MH, Ho JCM. Uni-axial Compression Test of Concrete-filled-steel-tube Columns Confined by Tie Bars. Procedia Engineering. 2013;57:662-9.
[16] Huang CS, Yeh Y-K, Liu G-Y, Hu H-T, Tsai KC, Weng YT et al. Axial Load Behavior of Stiffened Concrete-Filled Steel Columns. Journal of Structural Engineering. 2002;128:1222-30.
[17] Tao Z, Han L-H, Wang Z-B. Experimental behaviour of stiffened concrete-filled thin-walled hollow steel structural (HSS) stub columns. Journal of Constructional Steel Research. 2005;61:962-83.
[18] Tao Z, Han L-H, Wang D-Y. Strength and ductility of stiffened thin-walled hollow steel structural stub columns filled with concrete. Thin-Walled Structures. 2008;46:1113-28.
[19] Tao Z, Han L-H, Wang D-Y. Experimental behaviour of concrete-filled stiffened thin-walled steel tubular columns. Thin-Walled Structures. 2007;45:517-27.
[20] Alatshan F, Osman SA, Hamid R, Mashiri F. Stiffened concrete-filled steel tubes: A systematic review. Thin-Walled Structures. 2020;148:106590.
[21] Zheng M, Nie X, Ding R. Experimental and numerical research on the uniaxial behavior of the stiffened circular concrete-filled steel tube stub columns. Engineering Structures. 2024;306:117785.
[22] Singh H, Tiwary AK, Eldin SM, Ilyas RA. Behavior of stiffened concrete-filled steel tube columns infilled with nanomaterial-based concrete subjected to axial compression. Journal of Materials Research and Technology. 2023;24:9580-93.
[23] Zhou Z, Denavit MD, Zhou X. New cross-sectional slenderness limits for stiffened rectangular concrete-filled steel tubes. Engineering Structures. 2023;280:115689.
[24] Hassanein MF, Huang W-F, Shao Y-B, Cashell KA, Elsisy AR. Confinement-based design and behaviour of concrete-filled stiffened steel tubular square slender columns. Ocean Engineering. 2024;304:117845.
[25] Huang W-F, Shao Y-B, Hassanein MF, Hadzima-Nyarko M, Radu D, Cashell KA. Experimental and numerical investigation of square concrete-filled double-skin steel stiffened tubular stub columns with CHS inner tubes under axial compression. Thin-Walled Structures. 2024;199:111792.
[26] Zhou Z, Zhou X, Gan D, Liu Y. Comparison and design of stiffened rectangular concrete-filled steel tubular members. Journal of Constructional Steel Research. 2023;208:108037.
[27] Peng K, Yu T, Hadi MNS, Huang L. Compressive behavior of hybrid double-skin tubular columns with a rib-stiffened steel inner tube. Composite Structures. 2018;204:634-44.
[28] Zakir M, Sofi FA, Naqash JA. Experimentally verified behavior and confinement model for concrete in circular stiffened FRP-concrete-steel double-skin tubular columns. Structures. 2021;33:1144-57.
[29] Zakir M, Sofi FA, Naqash JA. Compressive testing and finite element analysis-based confined concrete model for stiffened square FRP-concrete-steel double-skin tubular columns. Journal of Building Engineering. 2021;44:103267.
[30] Zeng J-J, Liang S-D, Zhuge Y, Zhou J-K, Liao J. Seismic behavior of FRP-concrete-steel double skin tubular columns with a rib-stiffened Q690 steel tube and high-strength concrete.

Thin-Walled Structures. 2022;175:109127.
[31] Zeng J-J, Zheng Y-Z, Long Y-L. Axial compressive behavior of FRP-concrete-steel double skin tubular columns with a rib-stiffened Q690 steel tube and ultra-high strength concrete. Composite Structures. 2021;268:113912.
[32] Yu T, Teng JG, Wong YL. Stress-Strain Behavior of Concrete in Hybrid FRP-Concrete-Steel Double-Skin Tubular Columns. Journal of Structural Engineering. 2010;136:379-89.
[33] Ding F, Lu D, Lai Z, Liu X. Study on restraint coefficient of the stirrups-stiffened square concrete filled double-skin steel tube axial compression stub columns. Structures. 2024;60:105847.
[34] Zhang J-H, Hassanein MF, Cashell KA, Hadzima-Nyarko M, Xu Y, Shao Y-B. Experimental and numerical investigation on the behaviour of square concrete-filled cold-formed double-skin steel stiffened tubular short columns. Engineering Structures. 2024;303:117560.
[35] Zhang J-H, Shao Y-B, Hassanein MF, Cashell KA, Hadzima-Nyarko M. Behaviour of ultra-high strength concrete-filled dual-stiffened steel tubular slender columns. Engineering Structures. 2024;300:117204.
[36] Zhang J-H, Shao Y-B, Hassanein MF, Patel VI. Axial compressive performance of ultra-high strength concrete-filled dual steel tubular short columns with outer stiffened tubes and inner circular tubes. Journal of Constructional Steel Research. 2023;203:107848.
[37] Zhang J-H, Shao Y-B, Hassanein MF, Cashell KA, Hadzima-Nyarko M. Behaviour of cold-formed concrete-filled dual steel stiffened tubular short columns. Journal of Constructional Steel Research. 2024;213:108381.
[38] Wang Z-B, Tao Z, Yu Q. Axial compressive behaviour of concrete-filled double-tube stub columns with stiffeners. Thin-Walled Structures. 2017;120:91-104.
[39] Ghannam M, Metwally IM. Numerical investigation for the behaviour of stiffened circular concrete filled double tube columns. Structures. 2020;25:901-19.
[40] Wang Z-B, Zhang J-B, Li W, Wu H-J. Seismic performance of stiffened concrete-filled double skin steel tubes. Journal of Constructional Steel Research. 2020;169:106020.
[41] Hasan HG, Ekmekyapar T. Mechanical Performance of Stiffened Concrete Filled Double Skin Steel Tubular Stub Columns under Axial Compression. KSCE Journal of Civil Engineering. 2019;23:2281-92.
[42] Shekastehband B, Taromi A, Abedi K. Fire performance of stiffened concrete filled double skin steel tubular columns. Fire Safety Journal. 2017;88:13-25.
[43] Ghannam M, Song TY. Fire Resistance Design of Concrete-Filled Steel Tube Stub Columns. Fire Technology. 2021;57:911-42.
[44] Benzaid R, Mesbah HA. Circular and Square Concrete Columns Externally Confined by CFRP Composite: Experimental Investigation and Effective Strength Models. In: Intech, editor. Fiber Reinforced Polymers - The Technology Applied for Concrete Repair: INTECH; 2013. p. 167-201.
[45] Song X, Gu X, Li Y, Chen T, Zhang W. Mechanical Behavior of FRP-Strengthened Concrete Columns Subjected to Concentric and Eccentric Compression Loading. Journal of Composites for Construction. 2013;17:336-46.
[46] Campione G, Miraglia N, Papia M. Strength and strain enhancements of concrete columns confined with FRP sheets. Structural Engineering and Mechanics. 2004;18.
[47] Tabsh SW. Stress-Strain Model for High-Strength Concrete Confined by Welded Wire Fabric. Journal of Materials in Civil Engineering. 2007;19:286-94.
[48] ABAQUS. ABAQUS standard user's manual, Version 6.12. USA: Dassault Systèmes Corp., Providence, RI; 2012.
[49] Tao Z, Wang Z-B, Yu Q. Finite element modelling of concrete-filled steel stub columns under axial compression. Journal of Constructional Steel Research. 2013;89:121-31.
[50] Gardner L, Nethercot DA. Numerical Modeling of Stainless Steel Structural Components—A Consistent Approach. Journal of Structural Engineering. 2004;130:1586-601.
[51] Ellobody E, Young B. Structural performance of cold-formed high strength stainless steel columns. Journal of Constructional Steel Research. 2005;61:1631-49.
[52] Tao Z, Uy B, Han L-H, Wang Z-B. Analysis and design of concrete-filled stiffened thin-walled steel tubular columns under axial compression. Thin-Walled Structures. 2009;47:1544-56.
[53] Ayough P. Experimental and Numerical Investigations of the Compressive Behavior of Concrete-Filled Steel Tubular Columns [Ph.D.]. Malaysia: University of Malaya (Malaysia); 2022.
[54] Huang CS, Yeh YK, Liu GY, Hu HT, Tsai KC, Weng YT et al. Axial Load Behavior of Stiffened Concrete-Filled Steel Columns. Journal of Structural Engineering. 2002;128:1222-30.
[55] Eurocode-4_part1.1. Design of composite steel and concrete structures, Part 1-1: General rules and rules for buildings. London: BS EN 1994-1-1:2004. British Standards Institution; 2005.
[56] AISC-360-22. American Institute of Steel Construction: Specification for Structural Steel Buildings. 2022.
[57] AIJ. Architectural Institute of Japan (AIJ) Standard for Structural Calculation of Steel Reinforced Concrete Structures, 5th Ed. 2001.